

# Range resolved lidar for long distance ranging with sub-millimeter resolution

Mohammad Umar Piracha<sup>1</sup>, Dat Nguyen<sup>1</sup>, Dimitrios Mandridis<sup>1</sup>, Tolga Yilmaz<sup>2,3</sup>, Ibrahim Ozdur<sup>1</sup>, Sarper Ozharar<sup>1,4</sup> and Peter J Delfyett<sup>\*1</sup>

<sup>1</sup>CREOL, The College of Optics and Photonics, University of Central Florida, Orlando, FL 32816 USA

<sup>2</sup>Raydiance Inc. 2199 S. McDowell Blvd. Petaluma, CA 94954 USA

<sup>3</sup>Currently with Lockheed Martin-Aculight 22121 20th Ave SE Bothell, WA 98021 USA

<sup>4</sup>Currently with Center for Photonic Communication and Computing, Northwestern University, Evanston, IL 60208 USA

*\*delfyett@creol.ucf.edu*

**Abstract:** A lidar technique employing temporally stretched, frequency chirped pulses from a 20 MHz mode locked laser is presented. Sub-millimeter resolution at a target range of 10.1 km (in fiber) is observed. A pulse tagging scheme based on phase modulation is demonstrated for range resolved measurements. A carrier to noise ratio of 30 dB is observed at an unambiguous target distance of 30 meters in fiber.

©2010 Optical Society of America

**OCIS codes:** (280.3640) Lidar; (140.4050) Mode-Locked lasers; (120.0120) Instrumentation, measurement, and metrology; (280.0280) Remote sensing and sensors

---

## References and links

1. T. Fujii, and T. Fukuchi, *Laser Remote Sensing* (Boca Raton, Taylor & Francis, 2005).
  2. I. Coddington, W. C. Swann, L. Nenadovic, and N. R. Newbury, "Rapid and precise absolute distance measurements at long range," *Nat. Photonics* **3**(6), 351–356 (2009).
  3. H. Araki, S. Tazawa, H. Noda, Y. Ishihara, S. Goossens, S. Sasaki, N. Kawano, I. Kamiya, H. Otake, J. Oberst, and C. Shum, "Lunar Global Shape and Polar Topography Derived from Kaguya-LALT Laser Altimetry," *Science* **323**(5916), 897–900 (2009).
  4. B. W. Schilling, D. N. Barr, G. C. Templeton, L. J. Mizerka, and C. W. Trussell, "Multiple-return laser radar for three-dimensional imaging through obscurations," *Appl. Opt.* **41**(15), 2791–2799 (2002).
  5. M.-C. Amann, T. Bosch, R. Myllylä, and M. Rioux, "Laser ranging: a critical review of usual techniques for distance measurement," *Opt. Eng.* **40**(1), 10 (2001).
  6. R. Agishev, B. Gross, F. Moshary, A. Gilerson, and S. Ahmed, "Range-resolved pulsed and CWFM lidars: potential capabilities comparison," *Appl. Phys. B* **85**(1), 149–162 (2006).
  7. X. Sun, J. B. Abshire, M. A. Krainak, and W. B. Hasselbrack, "Photon counting pseudorandom noise code laser altimeters," *Proc. SPIE* **6771**, 677100.1 – 677100.9 (2007).
  8. P. A. Hiskett, C. S. Parry, A. McCarthy, and G. S. Buller, "A photon-counting time-of-flight ranging technique developed for the avoidance of range ambiguity at gigahertz clock rates," *Opt. Express* **16**(18), 13685–13698 (2008).
  9. C. J. Karlsson, F. A. A. Olsson, D. Letalick, and M. Harris, "All-fiber multifunction continuous-wave coherent laser radar at 1.55 μm for range, speed, vibration, and wind measurements," *Appl. Opt.* **39**(21), 3716–3726 (2000).
  10. R. Schneider, P. Thurmel, and M. Stockmann, "Distance measurement of moving objects by frequency modulated laser radar," *Opt. Eng.* **40**(1), 33–37 (2001).
  11. S. M. Beck, J. R. Buck, W. F. Buell, R. P. Dickinson, D. A. Kozlowski, N. J. Marechal, and T. J. Wright, "Synthetic-aperture imaging laser radar: laboratory demonstration and signal processing," *Appl. Opt.* **44**(35), 7621–7629 (2005).
  12. M. J. Halmos, "Synthetic aperture lidar with chirped modelocked waveform," US Patent 7505488, (2009).
  13. K. W. Holman, D. G. Kocher, and S. Kaushik, "MIT/LL development of broadband linear frequency chirp for high-resolution lidar," *Proc. SPIE* **6572**, 65720J.1 – 65720J.8 (2007).
  14. S. Lee, D. Mandridis, and P. J. Delfyett, Jr., "eXtreme chirped pulse oscillator operating in the nanosecond stretched pulse regime," *Opt. Express* **16**(7), 4766–4773 (2008).
- 

## 1. Introduction

Light detection and ranging (lidar) is used for various applications such as remote sensing, altimetry and imaging [1–4]. A lidar system can be implemented using several different

techniques [5]. Lidar systems based on the phase-shift measurement method offer high resolution but the modulo  $2\pi$  nature of the phase leads to range ambiguity. In time of flight (TOF) based lidars, short high power pulses of less than 6.7 ps duration are required for sub-millimeter resolution [5,6]. Narrow pulses require more bandwidth, which increases receiver noise. Furthermore, for unambiguous long distance measurements with TOF lidar systems, low pulse repetition frequencies (PRF) must be used to prevent aliasing. Recently, unambiguous, photon-counting range-finding has been demonstrated, but the maximum resolution was  $\sim 1$  cm [7,8].

Continuous wave frequency modulated (CWFM) lidars rely on linearly ramping the optical frequency of a laser and interfering the delayed echo signal with a reference signal to produce a beat frequency [6,9,10]. The performance of CWFM lidars is affected by the span, duration, and linearity of the optical frequency sweep. Beck et al. demonstrated a synthetic aperture laser radar employing a tunable laser source with  $\sim 1$  km coherence length, and a digital reference channel signal was used to correct for phase errors [11]. A mode-locked laser (MLL) that generates pulses that are chirped to the free spectral range limit (typically, only a few hundred MHz) has also been demonstrated [12]. For sub-millimeter resolution, optical bandwidths of hundreds of GHz are required. Recently Holman et al. demonstrated a 20 GHz sweep in 1  $\mu$ s from a MLL [13]. This method can be scaled to produce frequency sweeps over hundreds of GHz but the size, complexity and cost of such a system will be high.

In this paper, a new laser ranging technique is presented that employs a chirped fiber Bragg grating (CFBG) to generate temporally stretched, frequency chirped pulses from a MLL with 746 GHz of optical bandwidth. This enables sub-millimeter range resolution using pulses that may be several meters long. The narrow linewidth of the longitudinal modes of the MLL result in a coherence length of tens of kilometers which enables lidar operation at long range. Temporally stretched pulses offer the advantage of easy amplification to high optical power levels while minimizing fiber nonlinearities. The high PRFs of MLLs allow fast measurements. A pulse tagging scheme based on phase modulation is also implemented to resolve range ambiguities with sub millimeter resolution and with a 30 dB carrier to noise ratio (CNR).

## 2. Temporally stretched, frequency chirped lidar

### 2.1 Conceptual overview

The overlap of two identical, linearly chirped pulses that have a small separation between them results in a beat frequency ( $\Delta f$ ), as shown in Fig. 1. The dispersion (1651 ps/nm) of the chirped fiber Bragg grating (CFBG) can be expressed in terms of the optical frequency and duration of a pulse resulting in a value,  $S = 250$  MHz/mm. As the difference in the relative positions of the pulses increases, the beat tone shifts to higher frequencies at a rate of  $S = 250$  MHz/mm. The target distance ( $D$ ) is given by  $D = \Delta f / 2S$ .

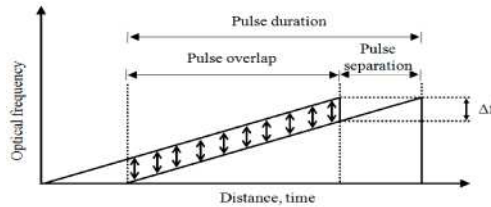


Fig. 1. The interference of a two identical, linearly chirped pulses generates a beat signal that depends on the relative distance between the overlapping pulses.

### 2.2 Experimental setup

The experimental setup of the lidar system is shown in Fig. 2. A 20 MHz mode-locked laser centered at a wavelength of 1553 nm is used to generate pulses of  $< 1$  ps duration (FWHM)

with a  $-3$  dB optical bandwidth of  $6$  nm ( $746$  GHz). A circulator is used to redirect the laser output to a CFBG with a dispersion of  $1651$  ps/nm, which imparts a wavelength dependent temporal delay on the optical pulses. This leads to a temporal stretching of the pulses to  $\sim 10$  ns (FWHM). Since the CFBG is not polarization maintaining, a polarizer is used to ensure polarization uniformity over the duration of the pulse.

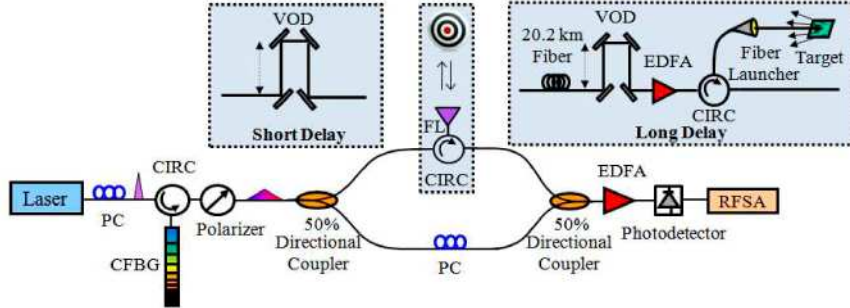


Fig. 2. Temporally stretched, frequency chirped lidar schematic. PC, Polarization Controller; CFBG, Chirped Fiber Bragg Grating; CIRC, Circulator; FL, Fiber Launcher; VOD, Variable Optical Delay; EDFA, Erbium Doped Fiber Amplifier; RFSA, RF Spectrum Analyzer.

A directional coupler splits the stretched pulses into a reference arm and a delay arm. A polarization controller in the reference arm is used to match the polarizations of the two arms. In the delay arm, a circulator and telescope can be used to launch and receive optical signals in free space. However, in the laboratory, measurements are made by simulating short or long target distances. For short range measurements, a free space variable optical delay (VOD) is used in the delay arm of the setup to introduce a relative path length difference between the two interferometer arms.

For long range measurements the long delay shown in Fig. 2 is used. It consists of a fiber spool and a VOD followed by an erbium doped fiber amplifier (EDFA). A circulator and fiber launcher are used to launch and receive pulses in free space. A flat metal plate is used as a target, located at a fixed distance of  $10$  cm from the fiber launcher. The reflected echo signal is received and combined with the reference optical signal that results in coherent detection at the photodetector, as described in section 2.1. Appropriate lengths of dispersion shifted fiber (DSF) and SMF-28 fiber are combined to create a total fiber delay of  $20.2$  km while minimizing fiber dispersion. However, due to the different dispersion slopes of the DSF and SMF-28 fibers, a residual dispersion exists which causes imperfections in the linearity of the chirp in the delay arm.

### 2.3 Short range lidar results

The stretched pulses have a duration of  $10$  ns (or  $2$  m in fiber), and a period of  $50$  ns (or  $10$  m in fiber). To ensure pulse overlap, the path length difference is kept below the temporal pulse length. The theoretically calculated and experimentally observed beat frequencies corresponding to different target distances are shown in Fig. 3(a). A CNR of  $> 30$  dB is observed. A closer examination of Fig. 3(a) reveals a broadening of the RF signal and a decrease in its magnitude as the delay is increased. Moreover, the envelope of the detected signal exhibits an undesirable modulation (noise) that is more prominent at longer delays. Simulations have confirmed that the group delay ripple (GDR) of the CFBG ( $< 50$  ps) causes a deviation from a perfectly linear chirp and deteriorates the shape and CNR of the beat signal. A technique similar to [11] may be used to correct for phase errors in the chirped waveform. The shift in beat frequency as a function of target distance reveals a dispersion,  $S = 484$  MHz/mm (or  $242$  MHz/mm in terms of round trip target distance) as shown in Fig. 3(b). It is in close agreement with theoretical value of the CFBG dispersion ( $250$  MHz/mm).

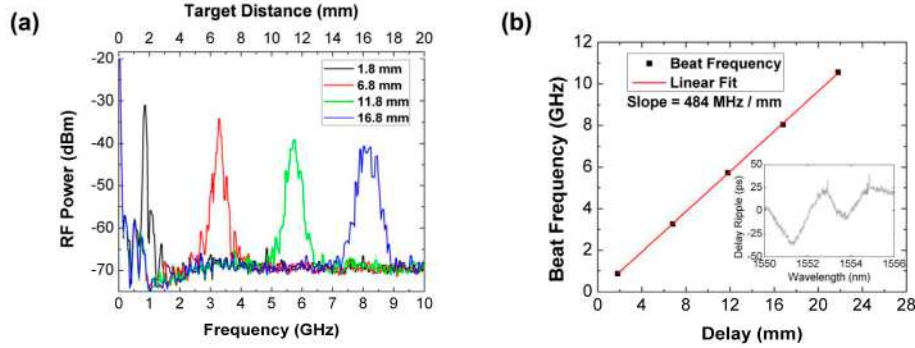


Fig. 3. a) Detected coherent heterodyned signals at different target distances b) Shift in the peak of the beat frequency as a function of target distance. Inset shows the GDR of the CFBG

#### 2.4 Long range lidar results

Long distance measurements are simulated in the laboratory using the experimental setup of Fig. 1 with 20.2 km of fiber delay. A relative fiber path length difference of 20.2 km leads to a temporal overlap of pulse 1 in the delay arm with the 2021<sup>st</sup> pulse in the reference arm. A beat signal with a  $-3$  dB width of  $\sim 200$  MHz is observed at a target distance of 1010 pulses + 1.3 mm, as shown in Fig. 4(a). A VOD is used to vary the target distance in 1 mm increments and the shift in the peak of the beat frequencies is recorded to reveal a CFBG dispersion slope of 466 MHz/mm, as shown in Fig. 4(b). We define the resolution of the lidar system as the  $-3$  dB width of the beat signal divided by the dispersion slope. The theoretical bandwidth limited lidar resolution is given by  $c / 2B$ , (where  $c$  = speed of light, and  $B$  = optical bandwidth in Hz) resulting in a value of 200  $\mu$ m. The fiber dispersion in the delay arm (as mentioned in section 2.2) has a detrimental effect on the lidar performance and a resolution of  $<500$   $\mu$ m at a target distance of 1010 pulses + 1.3 mm is observed.

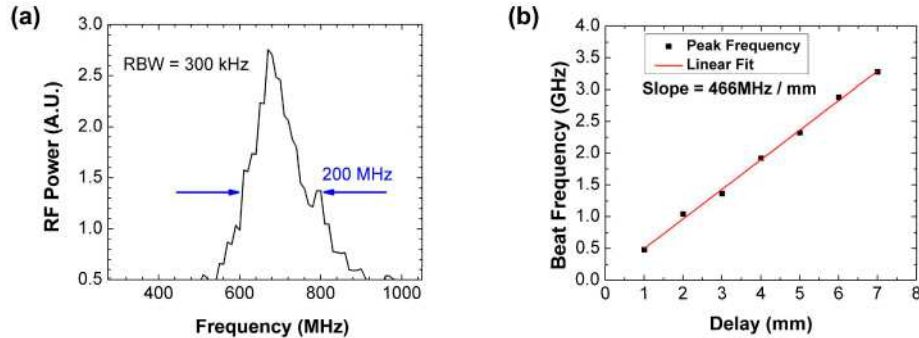


Fig. 4. a) Observed beat signal with a  $-3$  dB width of  $\sim 200$  MHz b) Shift in the peak of the beat frequency as a function of target distance.

In the current lidar configuration the 10 ns stretched pulses do not completely fill the 50 ns pulse period. To ensure pulse overlap, tuning the PRF of a 20 MHz MLL by 10 kHz, can shift the relative position between the two pulse trains by 50 ns at a range of 10.1 km. In addition to this, a laser with a larger optical bandwidth, a CFBG with higher dispersion, or a MLL with shorter time period (high PRF) can also be used to completely fill the time slots of the pulse train to ensure pulse overlap at all times [14].

### 3. Resolving the lidar range ambiguity

#### 3.1 Unambiguous range measurement using phase modulation

For unambiguous range measurements, a phase modulator driven by a frequency swept RF drive signal is used to modulate each pulse in the pulse train at a slightly different frequency. In Fig. 5, the difference in phase modulation frequencies between adjacent pulses is  $v_a$ , and the two pulse trains have a relative delay of “n” pulses. At the lidar receiver, the phase modulation side bands of the optical tones of the delayed and reference pulses generate a beat frequency at an offset of  $v_b = n \cdot v_a$  from the center tone.

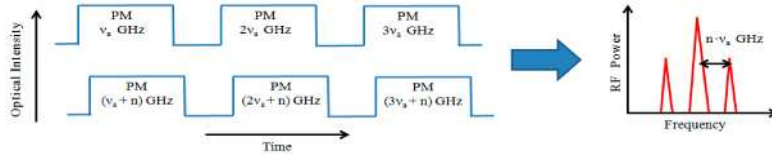


Fig. 5. Conceptual schematic of range resolved lidar operation.

The round trip delay (in terms of the number of pulses) is calculated by rounding off  $(v_b / v_a)$  to the nearest integer. The position of the center tone on the RF spectrum yields a target distance value that is added to the round trip delay value (in terms of number of pulses) to obtain the total round trip target distance.

#### 3.2 Generation of frequency swept RF drive signal

The RF drive signal for the phase modulator is generated by using two lasers (an HP-81682A narrow linewidth laser and a DFB laser) in a heterodyne configuration, shown in Fig. 6 (a). Figure 6 (b) shows the RF spectrum of the beat signal when the wavelengths of the two lasers are fixed at 1552 nm and 1552.022 nm respectively. A FWHM of ~22 MHz is observed.

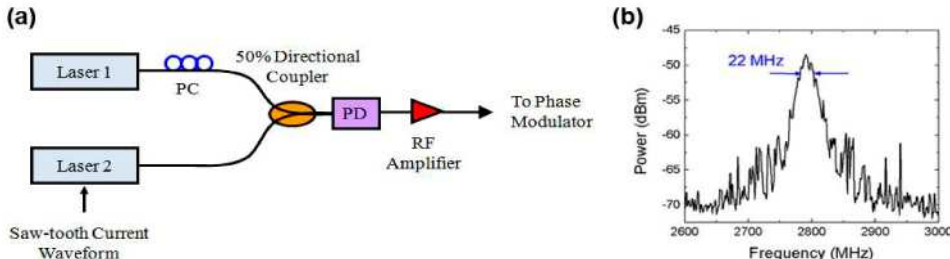


Fig. 6. a) Heterodyne schematic for frequency swept RF signal generation. PC, Polarization Controller; PD, Photodetector b) Beat signal generated from heterodyne setup.

To generate a frequency swept RF signal, a function generator is used to produce a saw-tooth current waveform. A diode driver generates a DC bias at 70 mA. The two signals are combined using a bias-tee and fed to the DFB laser in the heterodyne setup. The amplitude and period of the saw-tooth current waveform are adjusted to produce an RF beat signal that sweeps from 3 GHz to 10 GHz in 2.86  $\mu$ s (350 kHz). The difference in phase modulation frequency between adjacent pulses, (assuming the DFB has a perfectly linear frequency sweep) is given by  $v_a = F_s \cdot T_p / T_s$ , where  $F_s$  is the total span of the frequency sweep of the RF drive source,  $T_p$  is the period of the optical pulse, and  $T_s$  is the period of the sweep.

#### 3.3 Lidar setup for unambiguous range measurements

In Fig. 7, a phase modulator is introduced in the setup after the CFBG. It is driven by a frequency swept RF drive signal. Fifty seven optical pulses are phase modulated in single frequency sweep resulting in a maximum unambiguous round trip range of 570 m in fiber

(~855 m in free space). The linearity and slope of the DFB frequency sweep were characterized experimentally using a CWFM setup, revealing  $v_a = 167$  MHz/pulse. A broadband RF amplifier amplifies the frequency swept signal that drives the phase modulator.

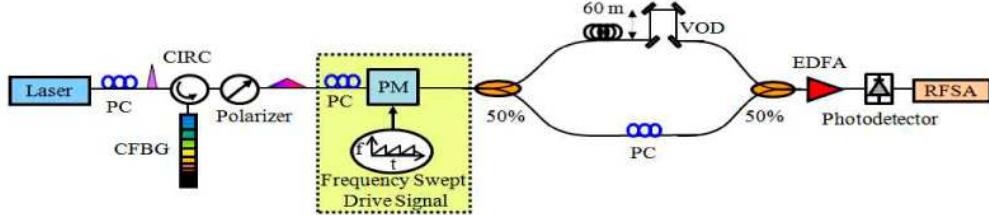


Fig. 7. Range Resolved Lidar Schematic. PM, Phase Modulator; PC, Polarization Controller; CFBG, Chirped Fiber Bragg Grating; CIRC, Circulator; VOD, Variable Optical Delay; EDFA, Erbium Doped Fiber Amplifier; RFSA, RF Spectrum Analyzer.

### 3.4 Results

A fiber delay of 60 m is used to simulate a round trip delay of 6 pulses as shown in Fig. 7. The VOD is then adjusted to add an additional free space round trip delay of 26.7 mm. In Fig. 8, the center heterodyne beat signal at 6.67 GHz corresponds to a round trip distance of 26.7 mm. A CNR of > 30 dB is observed. The phase modulation sidebands are observed at an offset of 1 GHz from the center tone, indicating a round trip delay of 6 pulses. Therefore the target round trip distance is 6 pulses plus a distance of 26.7 mm in free space. If the VOD is changed, the main beat note and sidebands shift while maintaining a 1 GHz spacing between them. Increasing the span, duration and linearity of the frequency swept RF drive signal by using a technique such as [13] will result in narrower side bands with larger CNR.

To ensure that the stretched pulses completely fill the time slots, a CFBG with large dispersion or a higher PRF can be used. Moreover, the difference in phase modulation frequency between adjacent pulses ( $v_a$ ) should be kept large enough to ensure that the main beat tone can be distinguished clearly from the sidebands. A large  $v_a$  and high PRF will increase the bandwidth requirement of the phase modulator. Therefore in a real system, the PRF,  $v_a$ , CFBG dispersion, and the phase modulator bandwidth have to be selected carefully.

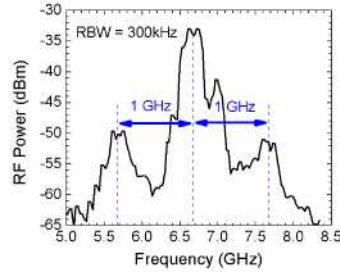


Fig. 8. Phase modulation sidebands at 1 GHz from the main tone.

## 5. Conclusion

A lidar setup employing a 20 MHz mode locked laser source is presented. A chirped fiber Bragg grating is used to generate temporally stretched, frequency chirped pulses. A target distance of ~15 km in air is simulated using optical fiber and sub-millimeter resolution is observed. For unambiguous range measurements, a heterodyne setup for generating a frequency swept RF signal is used for individually tagging pulses using phase modulation, at a simulated round trip target distance of ~90 m (in air) with > 30 dB CNR.